ISSN 1392–1320 MATERIALS SCIENCE (MEDŽIAGOTYRA). Vol. 19, No. 1. 2013

Current-Voltage Characteristics of the Metal / Organic Semiconductor / Metal Structures: Top and Bottom Contact Configuration Case

Šarūnas MEŠKINIS [1]*, Mindaugas PUCĖTA [1], Kęstutis ŠLAPIKAS [1], Sigitas TAMULEVIČIUS [1], Angelė GUDONYTĖ [1], Juozas Vidas GRAŽULEVIČIUS [2], Asta MICHALEVIČIŪTĖ [2], Tadas MALINAUSKAS [2], Jonas KERUCKAS [2], Vytautas GETAUTIS [2]

[1] *Institute of Materials Science of Kaunas University of Technology, Savanorių 271, LT-50131 Kaunas, Lithuania*
[2] *Kaunas University of Technology, Faculty of Chemical Technology, Radvilėnų 19, LT-50254 Kaunas, Lithuania*

crossref http://dx.doi.org/10.5755/j01.ms.19.1.3816

Received 25 June 2011; accepted 09 November 2011

In present study five synthesized organic semiconductor compounds have been used for fabrication of the planar metal / organic semiconductor / metal structures. Both top electrode and bottom electrode configurations were used. Current-voltage (I-V) characteristics of the samples were investigated. Effect of the hysteresis of the I-V characteristics was observed for all the investigated samples. However, strength of the hysteresis was dependent on the organic semiconductor used. Study of I-V characteristics of the top contact Al/AT-RB-1/Al structures revealed, that in (0 – 500) V voltages range average current of the samples measured in air is only slightly higher than current measured in nitrogen ambient. Deposition of the ultra-thin diamond like carbon interlayer resulted in both decrease of the hysteresis of I-V characteristics of top contact Al/AT-RB-1/Al samples. However, decreased current and decreased slope of the I-V characteristics of the samples with diamond like carbon interlayer was observed as well. I-V characteristic hysteresis effect was less pronounced in the case of the bottom contact metal/organic semiconductor/metal samples. I-V characteristics of the bottom contact samples were dependent on electrode metal used.

Keywords: organic semiconductor, metal-semiconductor contacts, spin coating, current-voltage characteristics, charge transport mechanism.

1. INTRODUCTION

Organic semiconductors remain under the significant attention due to the possibility to make electronic devices on large area flexible substrates (for example plastic or paper) using cheap technological processes such as spin coating and printing [1 – 4]. One of the main organic semiconductor based devices under development is organic field effect transistor (OFET). There are two main configurations of the OFET's [2, 3]. The first one is top contact configuration, where the source and drain electrodes are deposited on the top of the organic semiconductor. The second one is bottom contact configuration. In this case source and drain electrodes are beneath the organic semiconductor layer. For the top contact OFET's higher charge carrier mobility values are reported in comparison with the bottom contact OFET's [5, 6]. Therefore, most studies on the OFET fabrication and investigations are devoted to the top contact OFET's. On the other hand, bottom contact OFET configuration is more suited for integration into the low cost manufacturing process [7]. Such a configuration is compatible with "conventional" lithography techniques [7]: as a result OFET's with channel width as low as several tens of nanometers can be fabricated [8]. In the case of the bottom contact OFET's possible damage of the organic semiconductor layer during solution processing of the OFET electrodes can be avoided [7]. In addition, for successful implementation of the cheap organic electronics Devices, other important obstacles such as degradation of the OFET I-V characteristics due to the oxygen influence [9] as well as hysteresis of I-V characteristics should be solved [10, 11]. Interfacial effects in metal/organic semiconductor contacts should be considered [5 – 7].

In the present research, current-voltage (I-V) characteristics of the metal/organic semiconductor/metal structures fabricated using the five new organic semiconducting compounds were investigated. Air stability of organic semiconductors and effects of the diamond like carbon (DLC) interlayer has been investigated. I-V characteristics of the bottom and top contact configuration samples as well as samples fabricated using different organic semiconductors were compared.

2. EXPERIMENTAL

In the present study both top-contact and bottom-contact configuration of the samples have been used. All 3 configurations of the samples are presented in Fig. 1. The first configuration was square-shaped contact (electrode) on organic semiconductor. Second configuration of the samples – line shaped electrode on the top of the organic semiconductor. In this case, before the electrode metal evaporation, part of the organic semiconductor was removed in such a way, that ends of the line-shaped electrode were deposited directly onto the underlying dielectric layer. The third configuration used in present study was line-shaped electrodes beneath the organic semiconductor layer (bottom contact sample). In this case

*Corresponding author. Tel.: +370-37-327605; fax.: +370-37-314423.
E-mail address: *sarunas.meskinis@ktu.lt* (Š. Meškinis)

after the deposition of the organic semiconductor layer, part of it was subsequently removed exposing ends of the line-shaped electrodes (Fig. 1).

Monocrystalline wafers with thermally grown silicon dioxide (SiO_2) layers on the top were used as readily available substrates.

In the case of the top contact samples, the substrates were degreased in dimethylformamide and acetone. Afterwards organic semiconductor thin films were deposited by spin coating (deposition conditions are presented in Table 1). In all cases thickness of the organic semiconductor film was ~200 nm. Formation of the samples was finished by vacuum evaporation of the metal electrodes. 300 nm thickness Al films were deposited through the mask.

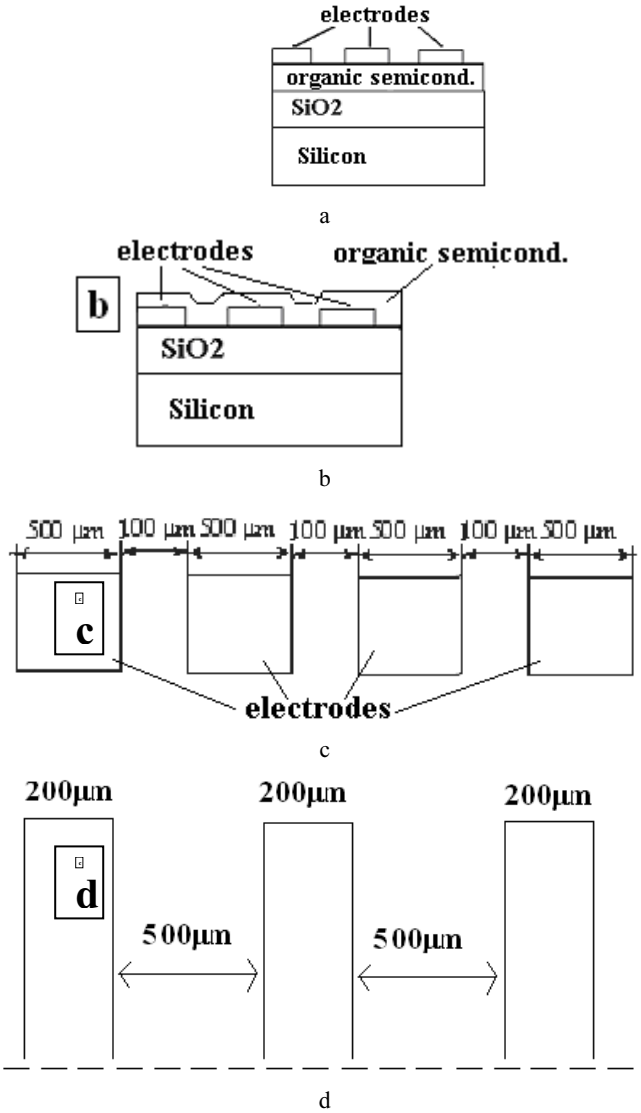

Fig. 1. Structure of the metal / organic semiconductor / metal samples used in present study: cross-section of the top contact samples (a), cross-section of the bottom contact samples (b), top view of the square-shaped electrodes (c), top view of the line-shaped electrodes (d)

Fabrication of the bottom contact samples began with degreasing of the substrates in dimethylformamide and acetone. Then samples as soon as possible were transferred to the vacuum evaporation chamber. 200 nm thickness metal electrodes were deposited through the mask. Afterwards samples were removed from vacuum chamber and organic semiconductor thin films were deposited by spin coating (deposition conditions are presented in Table 1).

Five organic semiconductors were investigated in the present study:

- 4-diphenylaminobenzaldehyde N-methyl-N-phenylhydrazone (further in the present study AT-RB-1);
- 4-diphenylaminobenzaldehyde N,N-diphenylhydrazone (further in the present study AT-RB-2);
- Olygomer – poly[9-(2,3-epoxypropylcarbazole] (further in the present study PEPK);
- Poly[4,4'-diformyltriphenylamine bis(N-2,3-epoxypropyl-N-phenylhydrazone) -alt-1,3-benzendithiol] (further in present study MT-16);
- 1,1-bis{4-[N,N-di(2-methoxyphenyl)]aminophenyl} cyclohexane (further in present study JK-17).

The synthesis of AT-RB-1 and AT-RB-2 has been described by Nomura et al in [12]. More information on PEPK can be found in [13]. The synthesis of the organic semiconductor MT-16 was reported in [14]. Compound JK-17 was prepared by Ulmann coupling of 1,1-bis(4-aminophenyl)cyclohexane with 2-iodoanisole. All organic semiconductors had p-type conductivity. The structures of organic semiconductors used in this study are shown in Fig. 2.

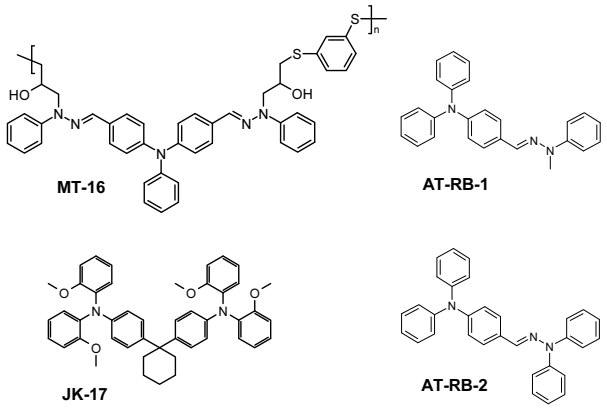

Fig. 2. Structures of compounds MT-16, JK-17, AT-RB-1, AT-RB-2

Current-voltage characteristics of the organic field effect transistors were investigated using a picoammeter/ /voltage source Keithley 6487. The measurements were performed in air. In some cases measurements were performed in nitrogen gas ambient.

Table 1. Parameters of the organic semiconductor thin film deposition process

Organic semicond.	Solvent	Solution formation temp.	Concentr. of the solution (%)	Spin coat. rate (rpm)
AT-RB-1	THF*	Room	5	6000
AT-RB-2	THF*	Room	5	6000
PEPK	THF*	Room	5	6000
JK-17	THF*	Room	5	6000
MT-16	THF*	Room	1.5	6000

* THF refers to the tetrahydrofurane.

Different charge transfer mechanisms in metal/organic semiconductor contacts were considered in present research. To define possible charge transfer mechanisms both contact limited (Schottky emission, Fowler-Nordheim emission, trap activated tunnelling) and bulk limited (space charge limited current, Poole-Frenkel emission) mechanisms were investigated.

Presence of the Schottky emission can be identified from the linear dependence of $\ln(J) \sim E^{1/2}$ [11, 15]. Presence of that charge transfer mechanism can be checked by comparison of the dielectric permittivity calculated from the Richardson equation with dielectric permittivity calculated from the capacitance-voltage measurement data, too.

Presence of the Fowler-Nordheim charge transfer mechanism can be identified from the linear dependence of $\ln(J/E^2) \sim E^{1/2}$ [11, 15].

Trap assisted tunnelling via traps at the metal/organic semiconductor interface is described by $\ln(J) \sim 1/E$ dependence [11, 16].

Space charge limited current is related with accumulation of the space charge in bulk of the semiconductor [11, 15]. It can be described by the $\log(J) \sim \log V$ ($\log(J) \sim \log(E)$) dependence. In such a case current density is dependent on the distance between the electrodes: the higher distance the lower current density will be detected.

Poole-Frenkel emission is related to trapping of the charge carriers by local traps related with bulk defects and subsequent release of the trapped charge carriers from these potential wells [11, 15]. The Poole-Frenkel emission can be identified by known dependence of the relation $ln(J/E) \sim E^{1/2}$. Presence of that charge transfer mechanism can be checked by comparison of the dielectric permittivity calculated from the equation (4) with the dielectric permittivity calculated from the capacitance-voltage measurement data, too.

3. EXPERIMENTAL RESULTS

3.1. Measurement ambient influence on current-voltage characteristics

Study on the influence of the measurement ambient on I-V characteristics of the top contact Al/AT-RB-1/Al structures revealed, that in 0 V – 500 V voltages range average current of the samples measured in air is slightly higher than current measured in nitrogen ambient (Fig. 3).

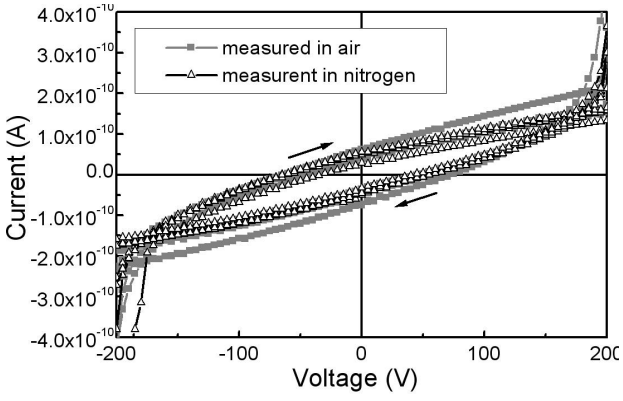

Fig. 3. The influence of the measurement ambient on I-V characteristics of sample Al/AT-RB-1/Al

Hysteresis was observed both for I-V characteristics measured in air and in nitrogen ambient. It means, that in the case of the organic semiconductor AT-RB-1 relatively good air stability was observed.

3.2. The influence of DLC interlayer

In present study the influence of the 5 nm thickness diamond like carbon (DLC) interlayer on I-V characteristics of top contact Al/AT-RB-1/Al sample was investigated. Hydrogenated diamond like carbon interlayer was deposited from acetylene gas by using closed drift ion source (ion beam energy 800 eV). The deposition was performed via mask before the vacuum evaporation of electrodes. More information on deposition and properties of diamond like carbon film can be found in [17].

Decreased dispersion of I-V characteristics in the case of the sample with diamond like carbon interlayer was observed (Fig. 4). Hysteresis of I-V characteristics decreased as well as a result of the insertion of diamond like carbon interlayer. However, decreased current and decreased slope of the I-V characteristics of the samples with diamond like carbon interlayer can be seen as well. It seems, that insertion of the DLC interlayer results in formation of the metal/insulator/semiconductor like structure.

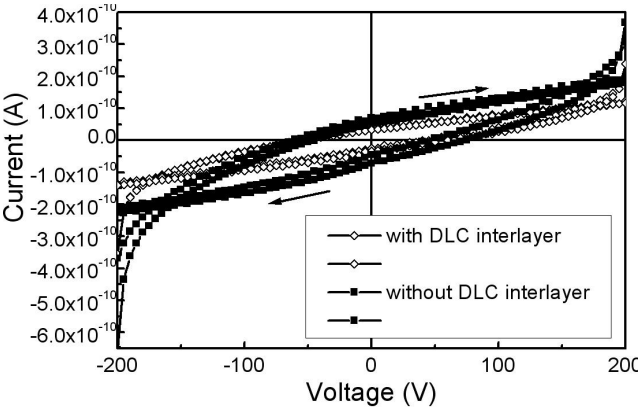

Fig. 4. The influence of 5 nm thickness diamond like carbon interlayer on I-V characteristics of Al/AT-RB-1/Al sample.

3.3. The influence of the contacting place on I-V characteristics of the top contact metal/ /organic semiconductor/metal samples

Top contact Al/AT-RB-1/Al samples with line shaped electrodes were investigated. In all cases I-V characteristics typical for double Schottky contact metal-semiconductor-metal structures were observed (Fig. 5). Significantly larger current in comparison with samples with square shaped electrodes can be seen. It can be explained by increased area of the electrodes. Hysteresis effect was observed for those samples. However in the case of the samples with line shaped electrodes only minor difference was observed between the zero bias current measured "forward" and "backward". It is different behavior in comparison with the samples with the square shaped electrodes (see Figs. 3, 4). In addition it should be mentioned, that in the case of the line shaped electrode samples, current measured "forward" is lower in

comparison with the "backwards" measured current (Fig. 5). While in the case of the samples with square shaped electrodes current measured "forward" is higher than current measured "backwards". It can be seen in Fig. 6, that I-V characteristic of the samples with line shaped electrodes depends on the placement of the contacting probe – wether the contacting place beneath the electrode is organic semiconductor or not. The main charge transfer mechanisms were considered for the samples with line shaped electrodes. It can be seen in Fig. 6, that the main charge transfer mechanism for the samples investigated is Schottky emission. While at higher voltages trap assisted tunneling and/or Fowler-Nordheim tunneling can be considered as well. Such a behaviour again is different from the samples with square shaped electrodes, where the main charge transfer mechanism was trap assisted tunneling and Schottky emission can be considered only at higher voltages [11]. It seems, that possible organic semiconductor deformation during the measurement of the I-V characteristics have significant influence on the measurement results.

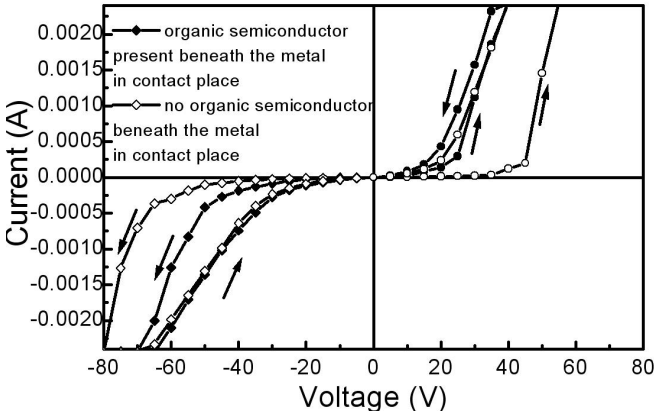

Fig. 5. I-V characteristics of top contact Al/AT-RB-1/Al samples with line shaped electrodes

3.4. Comparison of I-V characteristics of metal/organic semiconductor/metal samples with top contact and bottom contact configuration

I-V characteristics of the bottom contact metal/AT-RB-1/metal samples with line shaped electrodes are presented in Fig. 7. Quasilinear behaviour and very small hysteresis of I-V characteristic in comparison with the top contact samples was observed in the case of Al/AT-RB-1/Al samples. In the case of the bottom contact Ti/AT-RB-1/Ti samples slightly higher non-linearity and I-V hysteresis can be seen. It should be mentioned, that in the case of the top contact metal/AT-RB-1/metal samples smaller difference between the I-V characteristics of the samples with different electrode metal was observed [11]. It should be mentioned, that strong dependence of the bottom contact metal-organic semiconductor samples on electrode metal workfunction was reported in [18]. The influence of the possible metal surface oxidation before the deposition of the organic semiconductor layer should be taken into account as well (see eg. [19]).

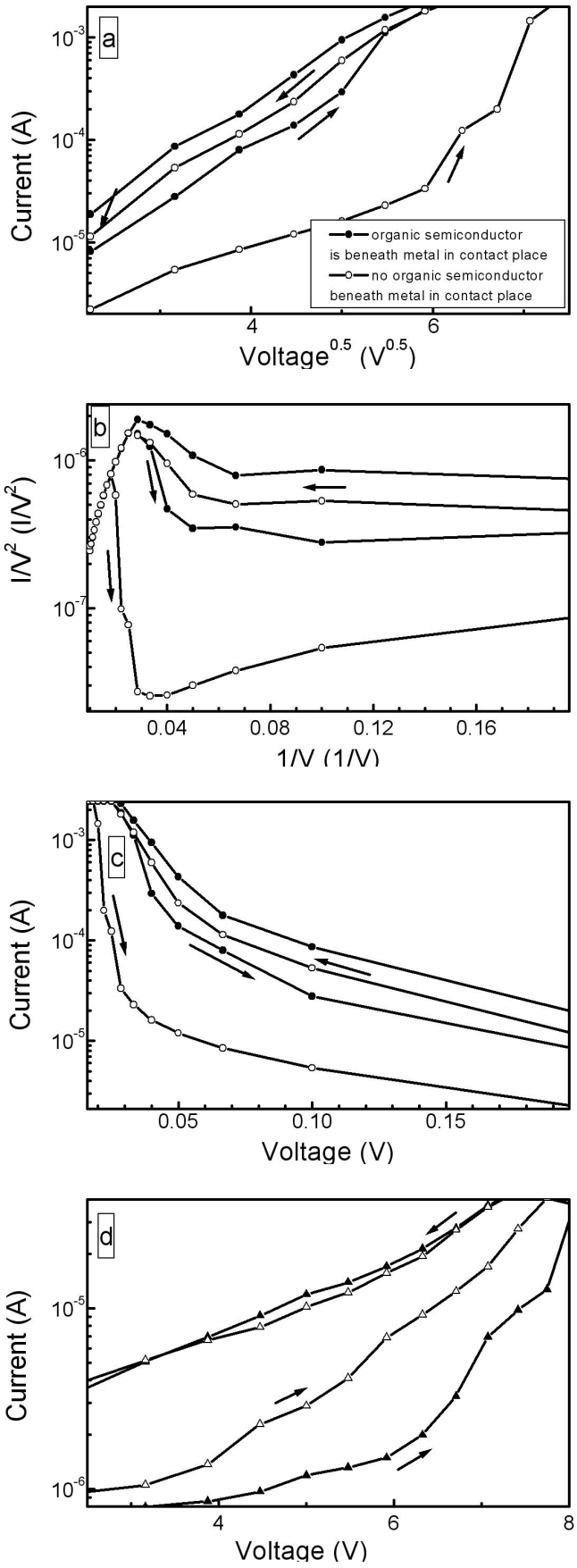

Fig. 6. Charge transfer in top contact Al/AT-RB-1/Al samples with line shaped electrodes: Schottky plot (a), Fowler-Nordheim plot (b), trap-activated tunneling plot (c), Poole-Frenkel plot (d)

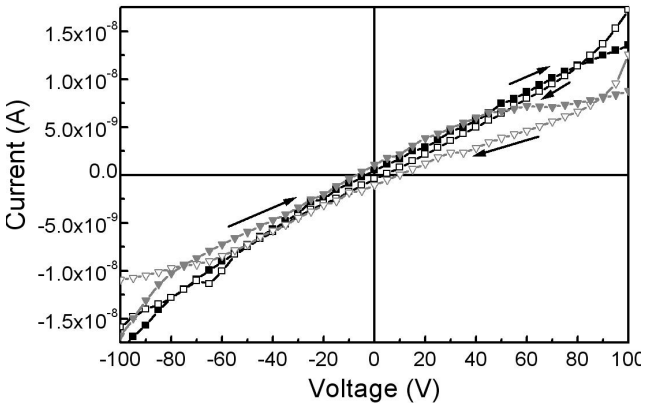

Fig. 7. I-V characteristics of bottom contact metal/AT-RB-1/metal samples with line shaped electrodes

Current-voltage characteristics of the bottom contact metal/AT-RB-2/metal samples were investigated as well. It can be seen in Fig. 8, that for Al/AT-RB-2/Al samples hysteresis of I-V characteristics is more pronounced than in the case of Al/AT-RB-1/Al samples. However, the behaviour of hysteresis is different – there is no considerable difference between the zero bias current for Al/AT-RB-2/Al samples. Negative resistance region can be seen in the case of the I-V characteristics of Al/AT-RB-2/Al samples. On the other hand, for bottom contact Cr/AT-RB-2/Cr samples quasilinear I-V characteristics with less pronounced hysteresis can be seen. It should be mentioned, that in the case of the top contact metal/AT_RB-2/metal samples assymetric I-V characteristics and big dispersion of the measurement results was observed [11].

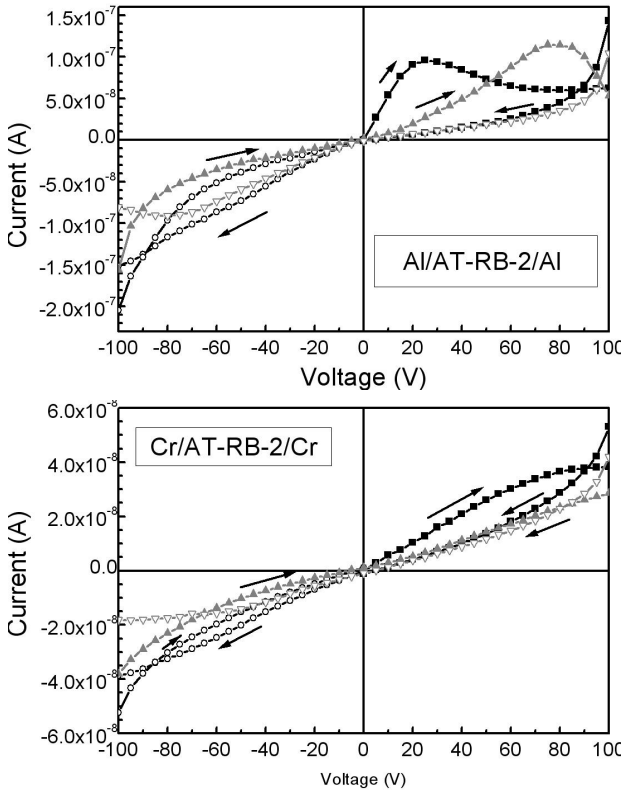

Fig. 8. I-V characteristics of bottom contact metal/AT-RB-2/metal samples with line shaped electrodes (electrode thickness 100 nm, line shaped electrode width belt width 200 μm, distance between the electrodes 500 μm)

I-V characteristics of bottom contact Al/PEPK/Al are presented in Fig. 9. In this case hysteresis of I-V characteristics is more pronounced than for Al/AT-RB-1/Al samples. Significant scattering of I-V characteristics should be mentioned. I-V characteristics of Al/JK-17/Al samples can be seen in Fig. 10. I-V hysteresis behaviour of these samples is more similar to Al/AT-RB-2/Al case. Negative resistance peaks (for some samples multiple) were observed.

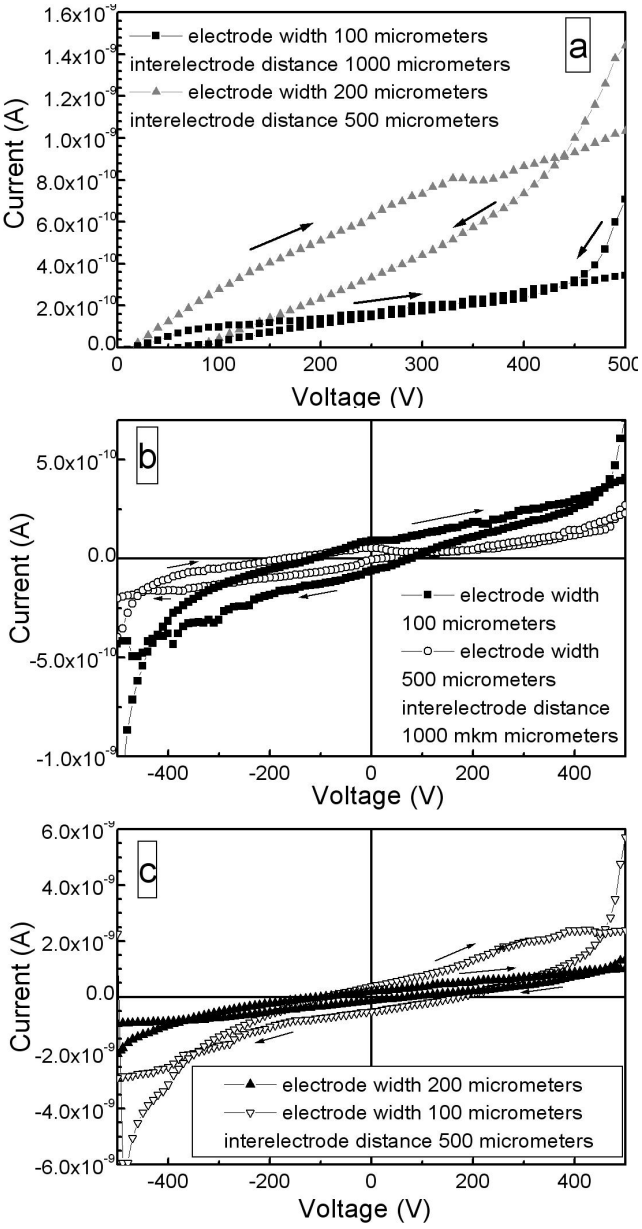

Fig. 9. I-V characteristics of bottom contact metal/PEPK/metal samples with line shaped electrodes – 0 V ÷ 500 V range (a), –500 V – +500 V range (b, c)

I-V characteristics of Al/MT-16/Al samples are presented in Fig. 11. Current voltage characteristics of Al/MT-16/Al structures can be grouped into two main types. In the first case hysteresis effect of the samples is even less pronounced than in the case of the bottom contact Al/AT-RB-1/Al samples. While in the second case some irregular negative resistance peaks can be seen.

I-V characteristics of the samples investigated were dependent on distance between the electrodes. It can be seen

in Fig. 10, that higher current was measured in the case of the smaller interelectrode distance. It means, that space charge limited current is one of the possible main charge transfer mechanisms in the case of the bottom contact samples along with metal/organic semiconductor interface related charge transfer mechanisms mentioned above.

The dependence of the sample's I-V characteristics on thickness of the electrode was investigated for Al/JK-17/Al samples (Fig. 11). It is difficult to say something about the possible influence of the electrode thickness due to the significant dispersion of the measurement results.

Decreased hysteresis in the case of the bottom contact samples in comparison with the top contact ones can be explained by taking into account the main possible mechanisms of the hysteresis of I-V characteristics in organic semiconductor based samples. Trap recharging, diffusion of mobile ions, formation and dissociation of bipolarons in the accumulation layer should be considered [20]. Particularly, in [21] larger I-V hysteresis in the case of the top contact sample in comparison with bottom contact ones was explained by formation of the effective potential barrier under the drain electrode due to the charging of the insulator interface.

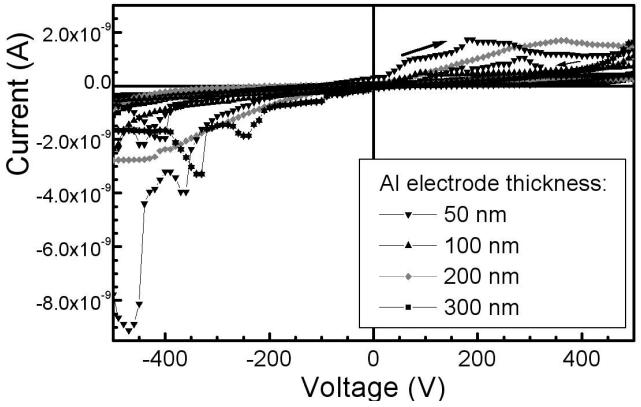

Fig. 10. I-V characteristics of bottom contact metal/JK-17/metal samples with line shaped electrodes

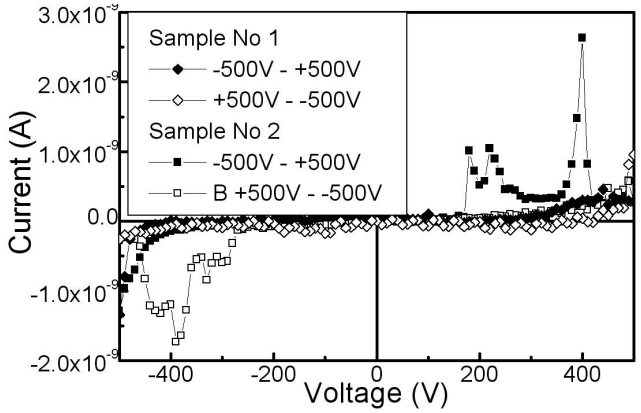

Fig. 11. I-V characteristics of bottom contact metal/MT-16/metal samples with line shaped electrodes

Considering nature of the negative resistance phenomena observed in present study for some samples it should be mentioned, that negative differential resistance effect was already reported for some organic semiconductor based structures [22 – 26]. Organic semiconductor based devices with bistable I-V characteristics containing negative differential resistance region was proposed as a possible memory devices [25, 26]. There are proposed two main explanations of the phenomena observed. The first one is trapping and de-trapping of carriers [22]. However, most authors it explain by presence of the some filamentary microconducting channels. In such a case at low voltages current flow via spatially localized pathways and as a result increased current strength is observed [22 – 26]. Subsequent current decrease at higher voltages is explained by to the strong local heating induced by current flowing via local microconducting channels [22]. In the case of the bottom-contact organic semiconductor devices not only bulk of the organic semiconductor, but organic semiconductor/ /electrode interface has significant influence on formation of the microconducting filament as well [24]. In addition the influence of the molecular length should be taken into account as well [27].

CONCLUSIONS

In conclusion I-V characteristics of the top contact and bottom contact metal/organic semiconductor/metal samples were studied. There were revealed, that in 0-500V voltages range average current of the top contact Al/AT-RB-1/Al structures only slightly depended on measurement environment. Current measured in air was slightly higher than current measured in nitrogen ambient. Deposition of the ultra-thin diamond like carbon interlayer resulted in both decrease of the hysteresis of I-V characteristics of top contact Al/AT-RB-1/Al samples. However, decreased current and decreased slope of the I-V characteristics of the samples with diamond like carbon interlayer was observed as well. I-V characteristic hysteresis effect was less pronounced in the case of the bottom contact metal/organic semiconductor/metal samples. Especially small hysteresis was in the case of the AT-RB-1 and MT-16 organic semiconductor based samples. I-V characteristics of the bottom contact samples depended on electrode metal used. For some bottom contact metal/organic semiconductor/ /metal samples based on AT-RB-2, MT-16 and JK-17 organic semiconductors negative resistance effect was observed.

Acknowledgments

This research was funded by a grant (No AUT-10/2010, High technologies development program project "Development and application of advanced holographic security means" (HOLOKID)) from the Research Council of Lithuania. Authors would like to thank Vitoldas Kopustinskas (Institute of Materials Science of Kaunas University of Technology) for deposition of the hydrogenated diamond like carbon interlayer.

REFERENCES

1. **Forrest, S. R.** The Path to Ubiquitous and Low-cost Organic Electronic Appliances on Plastic *Nature* 428 2004: pp. 911 – 918.
2. **Dimitrakopoulos, C. D., Malenfant, P. R. L.** Organic Thin Film Transistors for Large Area Electronics. *Advanced Materials* 14 2002: 99 – 117. http://dx.doi.org/10.1002/1521-4095(20020116)14:2<99::AID-ADMA99>3.0.CO;2-9

3. **Dimitrakopoulos, C. D., Mascaro, D. J.** Organic Thin-film Transistors: a Review of Recent Advances *IBM Journal of Research and Development* 45 2001: pp. 11 – 27.
4. **Misra, A., Kumar, P., Kamalasanan, M. N., Chandra, S.** White Organic LEDs and Their Recent Advancements *Semiconductor Science and Technology* 21 2006: pp. R35 – R47. http://dx.doi.org/10.1088/0268-1242/21/7/R01
5. **Cosseddu, P., Bonfiglio, A.** A Comparison between Bottom Contact and Top Contact All Organic Field Effect Transistors Assembled by Soft Lithography *Thin Solid Films* 515 2007: pp. 7551 – 7555.
6. **Yumiko Kaji, Ryoji Mitsuhashi, Xuesong Lee, Hideki Okamoto, Takashi Kambe, Naoshi Ikeda, Akihiko Fujiwara, Minoru Yamaji, Kenji Omote, Yoshihiro Kubozono.** High-performance C60 and Picene Thin Film Field-effect Transistors with Conducting Polymer Electrodes in Bottom Contact Structure *Organic Electronics* 10 2009: pp. 432 – 436.
7. **Facchetti, A.** Electroactive Oligothiophenes and Polythiophenes for Organic Field Effect Transistors *In Handbook of Tiophene based Materials: Applications in Organic Electronics and Photonics*. Eds. Perepichka, I. F., Perepichka, D. F.; Vol. 1, Print ISBN: 9780470057322, Online ISBN: 9780470745533, Wiley-Blackwell (an imprint of John Wiley & Sons Ltd), 2009: pp. 595 – 646.
8. **Haemori, M., Edura, T., Tsutsui, K., Itaka, K., Wada, Y., Koinuma, H.** Fabrication of Combinatorial Nm-planar Electrode Array for High Throughput Evaluation of Organic Semiconductors *Applied Surface Science* 252 2006: pp. 2568 – 2572.
9. **Tomoyuki Ashimine, Takeshi Yasuda, Masatoshi Saito, Hiroaki Nakamura, Tetsuo Tsutsui.** Air Stability of p-Channel Organic Field-Effect Transistors Based on Oligo-*p*-phenylenevinylene Derivatives *Japanese Journal of Applied Physics* 47 2008: pp. 1760 – 1762.
10. **Paasch, G., Scheinert, S., Herasimovich, A., Hörselmann, I, Lindner, Th.** Characteristics and Mechanisms of Hysteresis in Polymer Field-effect Transistors *Physica Status Solidi (a)* 205 2008: pp. 534 – 548. http://dx.doi.org/10.1002/pssa.200723400
11. **Meškinis, Š., Šlapikas, K., Gudaitis, R., Tamulevičius, S., Iljinas, A., Gudonytė, A., Gražulevičius, J. V., Getautis, V., Michalevičiūtė, A., Malinauska, T., Lygaitis, R.** Investigation of the Electrical Characteristics of the Metal/Organic Semiconductor/Metal Structures with Top Contact Configuration *Materials Science* (*Medžiagotyra*) 16 2010: pp. 195 – 201.
12. **Nomura, S., Nishimura, K., Shirota, Y.** Charge Transport in the Glassy State of Arylaldehyde and Arylketone Hydrazones *Thin Solid Films* 273 1996: pp. 27 – 34. http://dx.doi.org/10.1016/0040-6090(95)06766-3
13. **Gražulevičius, J. V., Strohriegl, P., Pielichowski, J., Pielichowski, K.** Carbazole-containing Polymers: Synthesis, Properties and Applications *Progress in Polymer Science* 28 2003: pp. 1297 – 1353. http://dx.doi.org/10.1016/S0079-6700(03)00036-4
14. **Getautis, V., Gražulevičius, J. V., Malinauskas, T., Jankauskas, V., Tokarski, Z., Jubran, N. L.** Novel Families of Hole-transporting Monomers and Polymers *Chemistry Letters* 33 2004: pp. 1336 – 1337.
15. **Gonon, P., Deneuville, A., Fontaine, F., Gheeraert, E.** Electrical Conduction and Deep Levels in Polycrystalline Diamond Films *Journal of Applied Physics* 78 1995: pp. 6633 – 6638.
16. **Houng, M. P., Wang, Y. H., Chang, W. J.** Current Transport Mechanism in Trapped Oxides: a Generalized Trap-assisted Tunneling Model *Journal of Applied Physics* 86 1999: pp. 1488 – 1491.
17. **Kopustinskas, V., Meškinis, Š., Tamulevičius, S., Andrulevičius, M., Čižiūtė, B., Niaura, G.** Synthesis of the Silicon and Silicon Oxide doped a-C:H Films from Hexamethyldisiloxane Vapor by DC Ion Beam *Surface & Coatings Technology* 200 2006: pp. 6240 – 6244.
18. **Rhee, Shi-Woo, Yun, Dong-Jin.** Metal-semiconductor Contact in Organic Thin Film Transistors *Journal of Materials Chemistry* 18 2008: pp. 5437 – 5444.
19. **Gundlach, D. J., Zhou, L., Nichols, J. A., Jackson, T. N., Necliudov, P. V., Shur, M. S.** An Experimental Study of Contact Effects in Organic Thin Film Transistors *Journal of Applied Physics* 100 2006: pp. 024509-1 – 024509-13.
20. **Paasch, G., Scheinert, S., Herasimovich, A., Hörselmann, I., Lindner, Th.** Characteristics and Mechanisms of Hysteresis in Polymer Field-effect Transistors *Physica Status Solidi (a)* 205 2008: pp. 534 – 548. http://dx.doi.org/10.1002/pssa.200723400
21. **Roichman, Y., Tessler, N.** Structures of Polymer Field-effect Transistor: Experimental and Numerical Analyses *Applied Physics Letters* 80 2002: pp. 151 – 153. http://dx.doi.org/10.1063/1.1431691
22. **Anjaneyulu, P., Sangeeth, C. S., Suchand, M. R.** Negative Differential Resistance in Doped Poly(3-methylthiophene) Devices *Journal of Physics D-Applied Physics* 43 2010: Article Number: 425103.
23. **Berleb, S., Batting, W., Schwoerer, M.** Anomalous Current-voltage Characteristics in Organic Light-emitting Devices *Synthetic Metals* 102 1999: pp. 1034 – 1037.
24. **Lebedev, E., Forero, S., Brütting, W., Schwoerer, M.** Switching Effect in Poly(*p*-phenylenevinylene) *Synthetic Metals* 111 – 112 2000: pp. 345 – 347.
25. **You, Y. T., Wang, M. L., Xuxie, H. N., Wu, B., Sun, Z. Y., Hou, X. Y.** Conductance-dependent Negative Differential Resistance in Organic Memory Devices *Applied Physics Letters* 97 2010: Article Number: 233301.
26. **Vilkman, M., Solehmainen, K., Laiho, A., Sandberg, H. G. O., Ikkala, O.** Negative Differential Resistance in Polymeric Memory Devices Containing Disordered Block Copolymers with Semiconducting Block *Organic Electronics* 10 2009: pp. 1478 – 1482.
27. **Yun Ren, Ke-Qiu Chen, Qing Wan, Anlian Pan, Hu, W. P.** Negative Differential Resistance in Polymer Molecular Devices Modulated with Molecular Length *Physics Letters A* 374 2010: pp. 3857 – 3862.